Influence of Large Metal Cations on the Photophysical Properties of Texaphyrin, a Rigid Aromatic Chromophore

Dirk M. Guldi,*,† Tarak D. Mody,‡ Nikolay N. Gerasimchuk,‡ Darren Magda,‡ and Jonathan L. Sessler*,§

Contribution from the Radiation Laboratory, University of Notre Dame, Notre Dame, Indiana 46556, Pharmacyclics, Inc., 995 East Arques Avenue, Sunnyvale, California 94086, and Department of Chemistry and Biochemistry, University of Texas at Austin, Austin, Texas 78712

Received May 8, 2000. Revised Manuscript Received June 16, 2000

Abstract: The excited-state properties, including singlet oxygen quantum yields, of a series of metallotexaphyrins (M-Tex), containing coordinated paramagnetic and also diamagnetic lanthanide(III) and other cations, are reported as are the solution-phase magnetic susceptibilities of the paramagnetic species. It is found that the singlet (1.593−1.638 eV) and triplet excited-state (1.478−1.498 eV) energies are only marginally affected by the choice of coordinated metal species. By contrast, photophysical parameters that are directly associated with the intrinsic decay rates of, for example, the singlet excited state, such as fluorescence lifetimes, reveal a strong dependence on the nature of the coordinated metal species. In particular, for the series of diamagnetic metals including Y−Tex, In−Tex, Lu-Tex, and Cd−Tex, an increase in atomic number leads to notably shorter lifetimes ($\tau_{\text{fluorescence}}$(Y-Tex) = 1298 ps, $\tau_{\text{fluorescence}}$(Lu-Tex) = 414 ps), a result that is interpreted as a heavy atom effect. The paramagnetic species, as a general rule, give rise to much shorter fluorescence lifetimes ($\tau_{\text{fluorescence}}$ = 99−515 ps) as compared to their diamagnetic analogues and are seen to fluoresce weakly, with fluorescence quantum yields (Φ_F = 0.0002−0.0028) that are at least 1 order of magnitude smaller than those found for the corresponding diamagnetic species (Φ_F = 0.015−0.04). Similar trends were also noted for the intersystem crossing rates and the triplet lifetimes, a finding that is interpreted in terms of an enhanced coupling between the singlet excited and triplet states or triplet excited and singlet ground states, respectively. The magnetic moments of the paramagnetic lanthanide(III) texaphyrin complexes were found to correlate well with the fluorescence lifetimes and the intersystem crossing rates, an observation that, along with other findings, including analyses of diamagnetic texaphyrin complexes, is considered consistent with the presence of covalent interactions between the texaphyrin ligand and the various coordinated metal centers.

Introduction

The investigation of metal complexes provides an experimental basis for understanding the effect of metal cations on the photophysical properties of coordinating ligands. In the specific case of the trivalent lanthanides, a class of cations made interesting by their obvious internal congruence in terms of charge (albeit not ionic radius or magnetic moment), such studies have been almost entirely limited to porphyrin-based complexes due to a generalized lack of ligands that provide 1:1 complexes of high kinetic stability.[1−6] The recent advent of metallotexaphyrins (M-Tex) is now changing this latter situation; these systems contain five nearly coplanar nitrogen donor atoms (cf. Figure 1) and form nonlabile 1:1 complexes with lanthanide(III) cations that are far superior to the corresponding porphyrin systems in terms of their kinetic stability.[7−10] In this paper, we report a detailed photophysical analysis of various metallotexaphyrins, including those of the lanthanide(III) series.[11] Briefly, in the case of the paramagnetic complexes derived from Nd(III), Sm(III), Eu(III), Gd(III), Tb(III), Dy(III), Ho(III), Er(III), Tm(III), and Yb(III), the triplet lifetimes and intersystem crossing rates are found to depend on the magnitude of the magnetic moment of the metal cation. In the case of the

† University of Notre Dame.

‡ Pharmacyclics, Inc.

§ University of Texas at Austin.

(1) Gouterman, M.; Schumaker, C. D.; Srivastava, T. S.; Yonetani, T. *Chem. Phys. Lett.* **1976**, *40*, 456−461.

(2) Tsvirko, M. P.; Stelmakh, G. F.; Pyatosin, V. E.; Solovyov, K. N.; Kachura, T. F.; Piskarskas, A. S.; Gadonas, R. A. *Chem. Phys.* **1986**, *106*, 467−476.

(3) Aaviksoo, J.; Freiberg, A.; Savikhin, S.; Stelmakh, G. F.; Tsvirko, M. P. *Chem. Phys. Lett.* **1984**, *111*, 275−278.

(4) Tsvirko, M. P.; Stelmakh, G. F.; Pyatosin, V. E.; Solovyov, K. N.; Kachura, T. F. *Chem. Phys. Lett.* **1980**, *73*, 80−83.

(5) Martarano, L. A.; Wong, C.-P.; Horrocks, W. D.; Goncalves, A. M. P. *J. Phys. Chem.* **1976**, *80*, 2389−2393.

(6) A considerable body of work has been devoted to exploring the "opposite problem", namely the effects of ligands on the absorption and luminescent properties of the lanthanide cations themselves. For a leading reference, see: Balzani, V.; Scandola, F. *Supramolecular Photochemistry*; Ellis Horwood: New York, 1991; pp 326−330. See also: Beitz, J. V. Similarities and Differences in Trivalent Lanthanide- and Actinide-ion Solution Absorption Spectra and Luminescence Studies. In *Handbook on the Physics and Chemistry of Rare Earths, Vol. 18—Lanthanides/Actinides: Chemistry*; Gschneider, K. A., Jr., Eyring, L., Choppin, G. R., Lander, G. H., Eds.; Elsevier Science BV: Amsterdam, 1994; pp 159−195.

(7) Sessler, J. L.; Mody, T. D.; Hemmi, G. W.; Lynch, V. *Inorg. Chem.* **1993**, *32*, 3175−3187.

(8) Sessler, J. L.; Hemmi, G.; Mody, T. D.; Murai, T.; Burrell, A.; Young, S. W. *Acc. Chem. Res.* **1994**, *27*, 43−50.

(9) Mody, T. D.; Sessler, J. L. Porphyrin and Expanded Porphyrin Based Diagnostic and Therapeutic Agents. In *Supramolecular Materials and Technologies*; Reinhoudt, D. N., Ed.; Wiley: New York, 1999; pp 245−294.

(10) Mody, T. D.; Fu, L.; Sessler, J. L. *Prog. Inorg. Chem.*, in press.

(11) For the results of an early preliminary study, see: Harriman, A.; Maiya, B. G.; Murai, T.; Hemmi, G.; Sessler, J. L.; Mallouk, T. E. *J. Chem. Soc., Chem. Commun.* **1989**, 314−316.

10.1021/ja001578b CCC: $19.00
Published on Web 08/06/2000

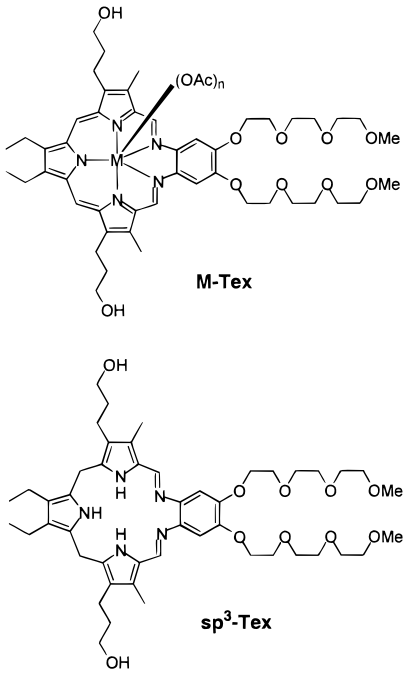

Figure 1. Compounds used in this study. For Cd-Tex, M = Cd and n = 1. For all other metallotexaphyrins complexes, Y-Tex, In-Tex, Lu-Tex, Nd-Tex, Sm-Tex, Eu-Tex, Gd-Tex, Tb-Tex, Dy-Tex, Ho-Tex, Er-Tex, Tm-Tex, Yb-Tex, n = 2 and M = Y, In, Lu, Nd, Sm, Eu, Gd, Tb, Dy, Ho, Er, Tm, and Yb, respectively.

diamagnetic Y(III), In(III), and Lu(III) complexes, the singlet lifetime, triplet lifetime, and intersystem crossing rate are found to correlate with the atomic number of the cation. We interpret these findings as evidence of covalency in the metal−texaphyrin bonding interactions.

While bearing important analogy to the porphyrins, the texaphyrins differ from these prototypical aromatic ligands in several important ways.[7−10] First, as noted above, they contain five, not four, nitrogen donor atoms. Second, they possess cores that are roughly 20% larger than those of the porphyrins and generally coordinate cations that are bigger. Third, they act as monoanionic, rather than dianionic, ligands when complexed to cationic metal centers. Finally, incorporating a Hückel aromatic periphery of 22 π-electrons (instead of 18 π-electrons), they possess a greater degree of aromatic delocalization and display spectral features, such as absorption and emission bands, that are substantially red-shifted compared to those of the porphyrins.

The lowest energy or Q-band maximum of texaphyrin complexes typically occurs around 730 nm,[7−10,12−15] a region where human tissues are relatively transparent.[16] This property has led to the development of the Lu(III) texaphyrin complex (Lu-Tex, motexafin lutetium; CAS Registry No. (provided by the author) 156436-90-7) as a photosensitizer for photodynamic therapy (PDT) of cancer, cardiovascular disease, and age-related macular degeneration.[9,10,12−15,17,18] The paramagnetic gadolinium(III) texaphyrin (Gd-Tex, motexafin gadolinium; CAS Registry No. (provided by the author) 156436-89-4), on the other hand, displayed no photodynamic activity in preclinical studies[19] and is currently in Phase III testing as a radiation therapy enhancer.[9,10,17,20] This observation provided the impetus for the current study, namely to understand the impact of the heavy metal atom and its associated spin state on the photophysical properties of the metallotexaphyrins. To this end, texaphyrin compounds, including most of the trivalent lanthanide series, as well as several analogous complexes, were examined using steady-state and fast kinetic techniques. Of major interest was the effect of the metal cation on the singlet excited-state lifetime, intersystem crossing, and triplet excited-state lifetime, insofar as these parameters largely determine the quantum yield of singlet oxygen formation in oxygenated systems.

While the large core size of the texaphyrins makes them ideally suited for the coordination of trivalent lanthanides, the inorganic chemistry of texaphyrins is not limited to this class of cations. For example, cadmium(II), yttrium(III), and indium(III) all form stable, well-characterized complexes and these species were thus included in this study. On the other hand, in marked contrast to the porphyrins, cation-free (so-called "free-base") texaphyrins appear to undergo rapid hydrolysis under protic conditions and therefore could not be subject to photophysical analysis.

Experimental Section

Synthesis. The Y(III), In(III), Lu(III), Eu(III), Gd(III), Dy(III), Tm(III), Yb(III), and Cd(II) complexes used in this study (Figure 1) have been described previously.[12,21] The syntheses of the Nd(III), Sm(III), Tb(III), Er(III), and Ho(III) complexes are described below. For this preparative work, solvents of reagent grade quality were purchased commercially and used without further purification. Metal salts were purchased from Alfa AESAR (Ward Hill, MA). LZY-54 zeolite was purchased from UOP (Des Plaines, IL). Ambersep 900 (OH) anion-exchange resin was purchased from Rohm and Haas Co. (Philadelphia, PA). Thin-layer chromatography (TLC) of the metallotexaphyrin complexes was carried out using a 4:1:2 v/v/v mixture of 1-butanol, acetic acid, and water, respectively, on Whatman K6F silica gel plates. Merck Type 60 (230−400 mesh) silica gel was used for column chromatography. For the purposes of initial characterization, electronic spectra were recorded on a Hitachi-U3000 spectrophotometer in methanol. All low- and high-resolution FAB and electrospray mass spectra were obtained from the University of California Mass Spectrometry Laboratory, Berkeley, CA. All elemental analyses were performed by Schwarzkopf Microanalytical Laboratory, Woodside, NY.

The purity of all new metallotexaphyrins employed in this study was established via HPLC analysis. The system employed was from Waters/Millipore and consisted of a 600E systems controller with a 510 pump, a 717 autosampler, and a 996 photodiode array detector. The detector monitored the elution profile from 250 to 800 nm. A C18 reversed-phase column was employed (Inertsil ODS2, 5 μM particle, from GL Science, Japan; packed by Metachem; the final column dimensions were 150 mm × 4.6 mm). All mobile-phase media were HPLC grade and obtained from Baxter. These mobile phases consisted of a 100 mM ammonium acetate buffer (pH adjusted to 4.3 with glacial acetic acid) and acetonitrile. The column was first eluted with 72%

(12) Young, S. W.; Woodburn, K. W.; Wright, M.; Mody, T. D.; Fan, Q.; Sessler, J. L.; Dow, W. C.; Miller, R. A. *Photochem. Photobiol*. **1996**, *63*, 892−897.

(13) Woodburn, K. W.; Fan, Q.; Miles, D. R.; Kessel, D.; Luo, Y.; Young, S. W. *Photochem. Photobiol*. **1997**, *65*, 410−415.

(14) Sessler, J. L.; Dow, W. C.; O'Connor, D.; Harriman, A.; Hemmi, G.; Mody, T. D.; Miller, R. A.; Qing, F.; Springs, S.; Woodburn, K.; Young, S. W. *J. Alloys Compd.* **1997**, *249*, 146−152.

(15) Woodburn, K. W.; Fan, Q.; Kessel, D.; Wright, M.; Mody, T. D.; Hemmi, G.; Magda, D.; Sessler, J. L.; Dow, W. C.; Miller, R. A.; Young, S. W. *J. Clin. Laser Med., Surg.* **1996**, *14*, 343−348.

(16) Wan, S.; Parrish, J. A.; Anderson, R. R.; Madden, M. *Photochem. Photobiol.* **1981**, *34*, 679−681.

(17) Sessler, J. L.; Miller, R. A. *Biochem. Pharmacol.* **2000**, *59*, 733−739.

(18) Blumenkranz, M. S.; Woodburn, K. W.; Qing, F.; Verdooner, S.; Kessel, D.; Miller, R. *Am. J. Opthalmol.* **2000**, *129*, 353−362.

(19) Grosswiner, L. I.; Biligin, M. D.; Berdusis, P.; Mody, T. D. *Photochem. Photobiol.* **1999**, *70*, 138−145.

(20) Miller, R. A.; Woodburn, K.; Fan, Q.; Renschler, M.; Sessler, J. L.; Koutcher, J. A. *Int. J. Biol. Radiat. Oncol.* **1999**, *45*, 981−989.

(21) Sessler, J. L.; Tvermoes, N. A.; Guldi, D. M.; Mody, T. D.; Allen, W. E. *J. Phys. Chem. A* **1999**, *103*, 787−794.

100 mM ammonium acetate buffer and 28% acetonitrile for 28 min. A linear gradient was then applied over the next 10 min to reach 20% 100 mM ammonium acetate buffer and 80% acetonitrile. The flow rate was 1.5 mL/min with the column temperature set at 40 °C.

General Procedure for the Synthesis of the Nd(III), Sm(III), and Tb(III) Complexes of Bis(acetato-*O*)[9,10-diethyl-20,21-bis[2-[2-(2-methoxyethoxy)ethoxy]ethoxy]-4,15-dimethyl-8,11-imino-3,6:16,13-dinitrilo-1,18-benzodiazacycloeicosine-5,14-dipropanolato-N^1, N^{18}, N^{23}, N^{24}, N^{25}] (i.e., Nd-Tex, Sm-Tex, and Tb-Tex). One equivalent of the hydrochloride salt of the so-called sp^3 texaphyrin precursor, 9,10-diethyl-7,12-dihydro-20,21-bis[2-[2-(2-methoxyethoxy)ethoxy]-ethoxy]-4,15-dimethyl-3,6:8,11:13,16-triimino-1,18-benzodiazacyclo-eicosine-5,14-dipropanol hydrochloride (sp^3-Tex; Figure 1),[12] 1.0−1.5 equiv of the relevant $M(OAc)_{n+1}\cdot xH_2O$ salt, and 10 equiv of triethylamine were mixed together in methanol (1 mL/4−40 mg of macrocycle) and heated to reflux while left exposed to air.[12] During the course of the reaction, air was periodically bubbled directly into the reaction vessel using a dispersion tube. The progress of the reaction was monitored by UV/vis spectroscopy and TLC. After the reaction was deemed complete, the deep green solution was cooled to room temperature, filtered through a pad of Celite, and stripped of solvent under reduced pressure. The resulting complex was then purified using the following procedure: (1) acetone trituration, (2) removal of free metal by zeolite extraction, (3) counterion exchange by acetic acid-washed Ambersep 900 resin, and (4) crystallization from a mixture of ethanol and *n*-heptane as described further below.

The crude metallotexaphyrin product, dark green solid, was suspended in acetone (25 mL/g of starting nonaromatic macrocycle), stirred for 30 min at room temperature, and then filtered to wash away the red/brown impurities (incomplete oxidation products and excess triethylamine). The resulting green solid was dried in vacuo. A weighed quantity of this material was then dissolved in MeOH using 35 mL of solvent/g of crude metallotexaphyrin complex, stirred for ∼30 min, and then filtered through Celite into a 1-L Erlenmeyer flask. Deionized water (3.5 mL/g of crude complex) was added to the flask along with LZY-54 zeolite that had been pretreated with acetic acid (5 g of zeolite/g of crude complex). The resulting mixture was agitated or shaken for 1−3 h and then filtered through Celite to remove the zeolite. This latter procedure, which constitutes a free metal extraction, was performed twice in order to ensure that the residual levels of free metal were low (i.e., <0.2 wt %). Once this process was complete, the filtrate was loaded onto a column (30 cm length × 2.5 cm diameter) of Ambersep 900 anion-exchange resin (pretreated so as to be in the acetate form) and eluted with MeOH. The eluent containing the bis-acetate complex was collected, concentrated to dryness under reduced pressure, and recrystallized from anhydrous ethanol/*n*-heptane (1:3 v/v) at 60 °C. The final product was collected by filtration on a fritted glass funnel and dried in vacuo at 40−45 °C for 24−48 h.

Nd-Tex(III). The sp^3 texaphyrin precursor (sp^3-Tex), in the form of its hydrochloride salt (2.0 g, 2.2 mmol), $Nd(OAc)_3\cdot xH_2O$ (1.3 g, 3.3 mmol), and triethylamine (2.03 g, 20.2 mmol) were mixed together in methanol (500 mL) and heated to reflux in the air. In accord with the general procedure described above, the reaction was deemed complete after 7 h. The solvent was removed under reduced pressure, and the solids were dried in vacuo. After acetone trituration, Nd-Tex complex (2.2 g) was loaded onto two Waters SepPak tC_{18} reversed-phase (10 g of sorbent) columns. Each column was pretreated first with methanol (500 mL) and then with 100 mM ammonium acetate (500 mL) prior to loading the crude Nd-Tex product. Toward this end, the crude Nd-Tex was dissolved in 15 mL of methanol and 45 mL of ammonium acetate (25 mM) and then adsorbed on the column. The column was washed with 100 mL of water to ensure removal of any free Nd(III) ion (i.e., uncomplexed cation). Then, the Nd-Tex product was isolated by eluting with neat methanol (50 mL). The dark green Nd-Tex complex was collected, the solvent removed under reduced pressure, and the solid dried in vacuo. It was further purified by silica gel chromatography by first using neat chloroform and then increasing concentrations of methanol in chloroform up to neat methanol. Purified Nd-Tex was collected. The solvent was removed under reduced pressure and the resulting solid dried in vacuo to afford 1.3 g (52%) of Nd-Tex as a dark green microcrystalline solid. For Nd-Tex: FAB MS, $[M - 2OAc^-]^+$, *m*/*z* 1017; HRMS, $[M - 2OAc^-]^+$, *m*/*z* 1016.3937 (calcd for $[C_{48}H_{66}{}^{145}NdN_5O_{10}]^+$, 1016.3973). Anal. Calcd for $[C_{48}H_{66}NdN_5O_{10}](OAc)_2(CHCl_3)$: C, 50.73; H, 5.86; N, 5.58. Found: C, 51.02; H, 6.18; N, 5.31.

Sm-Tex. The sp^3 texaphyrin precursor (sp^3-Tex),[12] in the form of its hydrochloride salt (3.0 g, 3.28 mmol), $Sm(OAc)_3\cdot 3H_2O$ (1.5 g, 3.94 mmol), and triethylamine (3.32 g, 32.8 mmol) were mixed together in methanol (300 mL) and heated to reflux in the air. In accord with the general procedure described above, the reaction was deemed complete after 3.5 h. After workup and recrystallization from ethanol/*n*-heptane as described above, 1.68 g (45%) of Sm-Tex was obtained in the form of a dark green microcrystalline solid. For Sm-Tex: FAB MS, $[M - 2OAc^- + H^+]^+$, *m*/*z* 1025; HRMS, $[M - 2OAc^-]^+$, *m*/*z* 1022.3983 (calcd for $[C_{48}H_{66}{}^{150}SmN_5O_{10}]^+$, 1022.3990); electrospray MS, [M − OAc], 1083. Anal. Calcd for $[C_{48}H_{66}SmN_5O_{10}](OAc)_2(H_2O)_2$: C, 53.04; H, 6.51; N, 5.95. Found: C, 53.10; H, 6.40; N, 5.80.

Tb-Tex. The sp^3 texaphyrin precursor (sp^3-Tex),[12] in the form of its hydrochloride salt (3.0 g, 3.28 mmol), $Tb(OAc)_3\cdot 4H_2O$ (1.60 g, 3.94 mmol), and triethylamine (3.32 g, 32.8 mmol) were mixed together in methanol (300 mL) and heated to reflux in the air. In accord with the general procedure described above, the reaction was deemed complete after 4 h. After workup and recrystallization from ethanol/*n*-heptane as described above, 2.94 g (78%) of Tb-Tex was obtained in the form of a dark green microcrystalline solid. For Tb-Tex: FAB MS, $[M - 2OAc^-]^+$, *m*/*z* 1032; HRMS, $[M - 2OAc^-]^+$, *m*/*z* 1031.4052 (calcd for $[C_{48}H_{66}TbN_5O_{10}]^+$, 1031.4063); electrospray MS, [M − OAc], 1091. Anal. Calcd for $[C_{48}H_{66}TbN_5O_{10}](OAc)_2$: C, 54.31; H, 6.31; N, 6.09; Tb, 13.82. Found: C, 54.20; H, 6.34; N, 5.806.03; Tb, 13.95.

Er-Tex. The sp^3 texaphyrin precursor (sp^3-Tex), in the form of its hydrochloride salt,[12] 1.00 g (1.09 mmol), $Er(OAc)_3\cdot XH_2O$ (0.57 g, 1.68 mmol), and triethylamine (2.07 g, 20.4 mmol) were mixed together in methanol (1000 mL) and heated to reflux in the air. In accord with the general procedure described above, the reaction was deemed complete after 12 h. After the solution was allowed to cool, the solvent and the triethylamine were removed under reduced pressure. The resulting residue (1.64 g) was redissolved in 50 mL of a 20% solution of methanol in aqueous 0.1 M ammonium acetate buffer (pH = 4.3) and loaded onto a 5-g Waters SepPak tC_{18} reversed-phase cartridge for purification. The purified Er-Tex complex was obtained in the form of seven consecutive fractions, of 50 mL each, that were eluted from the SepPak cartridge by using 35−45% CH_3OH in aqueous ammonium acetate as the mobile phase. The purity of the eluted complex in each of the seven fractions collected was confirmed via HPLC analysis. Accordingly, these seven fractions were combined, and the methanol was removed under reduced pressure at room temperature. The resulting solid was redissolved in an aqueous ammonium acetate (100 mM) buffer solution and loaded onto a 2-g SepPack tC_{18} reversed-phase column for desalting. The desalting procedure employed involved washing extensively with water and then eluting from the column using pure CH_3OH (60 mL) as the eluent. The yield of complex obtained in this way was 41% (0.52 g). For Er-Tex: λ_{max} (CH_3OH) 732, 474, 414, 354 nm; FAB MS, $[M - 2OAc^-]^+$, *m*/*z* 1038; HRMS, $[M - 2OAc^-]^+$, *m*/*z* 1038.4096 (calcd for $[C_{48}H_{66}{}^{166}ErN_5O_{10}]^+$, 1038.4113).; Anal. Calcd for $C_{52}H_{72}ErN_5O_{14}(H_2O)$: C, 53.09; H, 6.34; N, 5.95; Er, 14.22. Found: C, 52.80; H, 6.21; N, 5.94; Er, 14.19.

Ho-Tex. In analogy to what was used to prepare the Er(III) complex, the sp^3 texaphyrin precursor (sp^3-Tex), in the form of its hydrochloride salt,[12] (1.0 g, 1.09 mmol), $Ho(OAc)_3\cdot xH_2O$ (0.58 g, 1.70 mmol), and triethylamine (2.07 g, 20.4 mmol) were mixed together in methanol (1100 mL) and heated to reflux in the air. The reaction was deemed complete after 12 h. Normal workup (i.e., SepPak purification and desalting) then produced 0.905 g (72% yield) of the Ho-Tex complex. For Ho-Tex: λ_{max} (CH_3OH) 734, 474, 414, 350, 318 nm; FAB MS, $[M - 2OAc^-]^+$, *m*/*z* 1037; HRMS, $[M - 2OAc^-]^+$, *m*/*z* 1037.4121 (calcd for $[C_{48}H_{66}HoN_5O_{10}]^+$, 1037.4113). Anal. Calcd for $C_{52}H_{72}HoN_5O_{14}(H_2O)$: C, 53.19; H, 6.35; N, 5.96; Ho, 14.14.05. Found: C, 53.21; H, 6.11; N, 5.89; Ho, 14.11.

Photophysical Analysis. General Techniques. All optical measurements were performed on aqueous solutions containing 5% Tween 20, under conditions where the texaphyrin Q-band absorbance is concentration-independent and the complex is presumably monomeric.[19] Absorp-

tion spectra were recorded with a Milton Roy Spectronic 3000 array spectrophotometer. Emission spectra were recorded on an SLM 8100 spectrofluorometer. Fluorescence spectra were measured at room temperature. The excitation wavelength was adjusted to the metallotexaphyrin (M-Tex) ground-state absorption (around 730 nm). A long-pass filter in the emission path was used in order to eliminate the interference from the solvent and stray light. Long integration times (20 s) and low increments (0.1 nm) were applied. The slits were 2 and 8 nm. Each spectral plot used for subsequent analysis was constructed from an average of at least five individual scans.

Laser Flash Photolysis. Picosecond laser flash photolysis experiments were carried out with 532-nm laser pulses from a mode-locked, Q-switched Quantel YG-501 DP Nd:YAG laser system (pulse width ~18 ps, 2−3 mJ/pulse). The white continuum picosecond probe pulse was generated by passing the fundamental output through a D_2O/H_2O solution. The excitation and the probe pulses were fed to a spectrograph (HR-320, ISDA Instruments, Inc.) with fiber-optic cables and were analyzed with a dual diode array detector (Princeton Instruments, Inc.) interfaced with an IBM-AT computer. Picosecond kinetic time−absorption profiles represent an average wavelength region taken over ca. 10 nm. Nanosecond laser flash photolysis experiments were performed with laser pulses from a Molectron UV-400 nitrogen laser system (337.1 nm, 8 ns pulse width, 1 mJ/pulse) in a front face excitation geometry.[22]

Fluorescence lifetimes were measured with a laser strobe fluorescence lifetime spectrometer (Photon Technology International) with 460-nm laser pulses from a nitrogen/dye laser fiber-coupled to a lens-based T-form sample compartment equipped with a stroboscopic detector. Details of the laser strobe systems are described on the manufacturer's web site, http://www.pti-nj.com.

Singlet oxygen quantum yields (Φ_Δ) were measured by comparing the amplitude of $^1O_2$ phosphorescence at 1270 nm[23] with that generated by a known singlet oxygen sensitizer, namely, [60]fullerene.[24]

Magnetic Moments. Magnetic susceptibilities in solution were determined using the NMR method developed by Evans[25] and others.[26,27] Coaxial NMR tubes were used, with the solution of paramagnetic complex in the outer (5 mm) NMR tube and deuterated solvent (CD_3-OD) in the inner tube. Corrections for solvent[28] and diamagnetic Pascal atomic and bond increments[29] were used in the calculation of molar susceptibility and magnetic moments. Values of μ_{eff} are reported as the average and standard deviation of three independent experiments.

Results

Absorption Spectra. The singlet ground-state absorption spectra of all investigated metallotexaphyrins, recorded in 5% aqueous Tween, display two sets of strong transitions, reminiscent of those found in metalloporphyrin systems (Figure 2). Using Lu-Tex as an example, the visible region between 360 and 510 nm was found to be dominated by two high-intensity absorptions at 413 and 475 nm with $\epsilon = 47\,000\ M^{-1}\ cm^{-1}$ and $\epsilon = 125\,000\ M^{-1}\ cm^{-1}$, respectively. In the 650−810-nm region a series of Q-type transitions are observed with two major bands at 668 nm ($\epsilon = 11\,000\ M^{-1}\ cm^{-1}$) and 730 nm ($\epsilon = 38\,000\ M^{-1}\ cm^{-1}$), separated by a poorly resolved shoulder around 710 nm. Similar maxima and extinction coefficients were noted for all lanthanide(III) complexes; however, traversing the series from Nd(III) to Lu(III) leads to a small, but significant, blue-shift in both the high-energy and Q-like bands. The total difference in either band amounts to ca. 8 nm. Y(III) texaphyrin (736 nm) is similar to Dy(III) (737 nm), whereas the Cd(II) and In(III) complexes display absorbance maxima red-shifted by <5 nm relative to those of Lu-Tex.

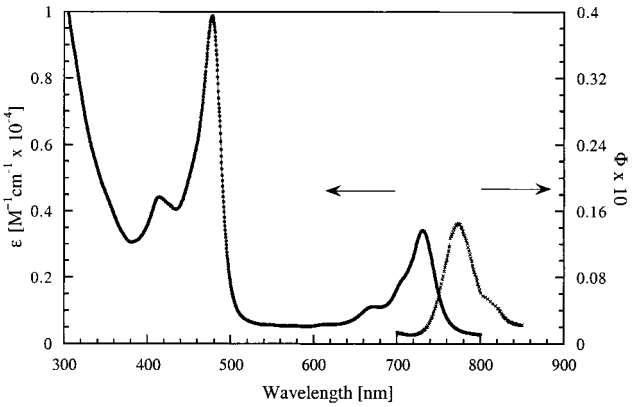

Figure 2. Absorption and fluorescence spectrum of Lu-Tex (motexafin lutetium) in aqueous solutions (5% Tween 20) at 298 K; excitation wavelength 473 nm.

Emission Spectra. The fluorescence emission spectrum of Lu-Tex (2.0×10^{-5} M, Figure 2) reflects nearly exactly the same ground-state absorption features as seen in the visible region. This similarity suggests that the distribution of vibrational levels in the singlet excited state resembles that of the ground state. The match of the two respective extreme lines, i.e., the absorption at the longest wavelength and the corresponding emission at the shortest wavelength, is good and is considered consistent with these features being assigned to zero−zero transitions between the ground and singlet excited states. A careful analysis reveals that the respective (*0 → 0) emission and (0 → *0) absorption bands differ slightly in energy (1.603−1.636 eV). The difference in observed maxima at 732 nm (absorption) and 772 nm (emission) can be interpreted in terms of a Stokes shift, involving inter alia energetic compensation for adjustment of the Lu-Tex singlet excited state to the new solvent environment. The observed Stokes shift is in reasonable agreement with those observed for other, e.g., porphyrin−metal, complexes.[30]

The fluorescence spectra of the other metallotexaphyrins exhibit structural patterns comparable to those described for Lu-Tex (cf. Table 1 for a summary of findings). As was true for the absorption bands, changes in the choice of coordinated metal center give rise to small, albeit detectable, shifts in the corresponding (*0 → 0) transitions (Y-Tex, 773 nm; Eu-Tex, 756 nm). However, because these changes are relatively small, it may be safely inferred that the singlet excited states energies are all similar.

In sharp contrast to the general similarities in excited singlet-state energies, the fluorescence quantum yields (Φ_F) of the various studied metallotexaphyrins, determined relative to a ZnTPP reference model in toluene ($\Phi_F = 0.04$),[31] show a dramatic dependence on the choice of the coordinated metal center (Table 1). In fact, these quantum yield values range from 0.0002 for the weakly fluorescent neodymium complex, Nd-Tex, to 0.04 for the much more strongly emitting yttrium complex, Y-Tex. In general, greater fluorescence is observed for diamagnetic complexes (cf. Discussion section below).

(22) Thomas, M. D.; Hug, G. L *Comput. Chem. (Oxford)* **1998**, *22*, 491−498.
(23) Rodgers, M. A. J.; Snowden, P. T. *J. Am. Chem. Soc.* **1982**, *104*, 5541−5543.
(24) Da Ros, T.; Prato, M. *Chem. Commun.* **1999**, 663−664.
(25) Evans, D. F. *J. Chem. Soc.* **1959**, 2003.
(26) Crawford, T. H.; Swanson, J. *J. Chem. Educ.* **1971**, *48*, 382−386.
(27) Ostfeld, D.; Cohen, I. A. *J. Chem. Educ.* **1972**, *49*, 829.
(28) *CRC Handbook of Chemistry and Physics*, 63rd ed.; Weast, R. C., Astle, M. J., Eds.; CRC Press: Boca Raton, FL, 1982.
(29) Drago, R. S. *Physical Methods in Chemistry*; W. B. Saunders Co.: Philadelphia, PA, 1977.
(30) Gouterman, M. Optical Specta and Electronic Structure. In *The Porphyrins, Vol. III*; Dolphin, D., Ed.; Academic Press: New York, 1978; pp 1−165.
(31) Murov, S. L.; Carmichael, I.; Hug, G. L. *Handbook of Photochemistry*; Marcel Dekker: New York, 1993.

Table 1. Spectroscopic and Photophysical Data of the Singlet Excited States (^{1}*M-Tex) of Water-Soluble M-Tex Complexes

	electron config	atomic no.	ionic radius (Å)[a]	Soret-band (nm)	Q-band (nm)	magnetic moment (B.M.)	fluorescence maxima (nm)	singlet energy (eV)	Φ_F	lifetime (fluor.) (ps)	ISC (s^{-1})
Y-Tex	$4p^6$	39	1.075	474	736	−	773	1.603	0.04	1298	0.605×10^9
Cd-Tex	$4d^{10}$	48	1.10[b]	469	733	−	770	1.609	0.015	715	1.48×10^9
In-Tex	$4d^{10}$	49	0.92[b]	471	731	−	768	1.613	0.032	1149	0.957×10^9
Lu-Tex	$4f^{14}$	71	1.032	477	730	−	772	1.605	0.015	414	1.89×10^9
Nd-Tex	$4f^3$	60	1.163	474	740	2.97 ± 0.02	757	1.636	0.0002	515	0.819×10^9
Sm-Tex	$4f^5$	62	1.132	474	742	2.43 ± 0.29	778	1.593	0.0005	420	1.5×10^9
Eu-Tex	$4f^6$	63	1.120	472	740	3.57 ± 0.11	756	1.638	0.0006	288	2.31×10^9
Gd-Tex	$4f^7$	64	1.107	473	739	7.96 ± 0.15	768	1.613	0.0028	208	3.77×10^9
Tb-Tex	$4f^8$	65	1.095	473	739	9.24 ± 0.09	772	1.604	0.0005	154	4.42×10^9
Dy-Tex	$4f^9$	66	1.083	474	737	10.25 ± 0.1	760	1.630	0.0004	99	15.6×10^9
Ho-Tex	$4f^{10}$	67	1.072	475	737	9.93 ± 0.09	770	1.609	0.0017	<100	18.3×10^9
Er-Tex	$4f^{11}$	68	1.062	474	736	9.33 ± 0.03	769	1.611	0.0011	<100	10.9×10^9
Tm-Tex	$4f^{12}$	69	1.052	477	733	8.20 ± 0.01	760	1.630	0.0009	161	9.33×10^9
Yb-Tex	$4f^{13}$	70	1.042	477	732	4.94 ± 0.33	757	1.636	0.0018	247	3.17×10^9

[a] Ionic radii were extracted from Shannon, R. D. *Acta Crystallogr.* **1979**, *A32*, 751−767, for nine-coordinate complexes. [b] Ionic radii for eight-coordinate complexes.

Table 2. Spectroscopic and Photophysical Data of the Triplet Excited States (^{3}*M-Tex) of Water-Soluble M-Tex Complexes

	electron config	atomic no.	ionic radius (Å)[a]	magnetic moment (B.M.)	phosphorescence maxima (nm)	triplet energy (eV)	Φ_T	λ_{max} (triplet) (nm)	$\epsilon_{triplet}$ (M^{-1} cm^{-1})	lifetime (triplet) (μs)
Y-Tex	$4p^6$	39	1.075	−	838	1.478	0.563	490	21500	187
Cd-Tex	$4d^{10}$	48	1.10[b]	−	827	1.498	0.25	500	24 000	122
In-Tex	$4d^{10}$	49	0.92[b]	−	830	1.492	0.50	500	14 100	126
Lu-Tex	$4f^{14}$	71	1.032	−	827	1.498	0.344	510	20 400	35.0
Nd-Tex	$4f^3$	60	1.163	2.97 ± 0.02	*c*	*d*	n.m.	510	*e*	n.m.
Sm-Tex	$4f^5$	62	1.132	2.43 ± 0.29	*c*	*d*	n.m.	520	*e*	n.m.
Eu-Tex	$4f^6$	63	1.120	3.57 ± 0.11	830	1.492	0.09	500	11 500	6.98
Gd-Tex	$4f^7$	64	1.107	7.96 ± 0.15	832	1.489	0.156	510	27 500	1.11
Tb-Tex	$4f^8$	65	1.095	9.24 ± 0.09	*c*	*d*	n.m.	515	*e*	<0.2
Dy-Tex	$4f^9$	66	1.083	10.25 ± 0.1	*c*	*d*	n.m.	520	*e*	0.00094
Ho-Tex	$4f^{10}$	67	1.072	9.93 ± 0.09	*c*	*d*	n.m.	515	*e*	0.00085
Er-Tex	$4f^{11}$	68	1.062	9.33 ± 0.03	*c*	*d*	n.m.	515	*e*	0.00076
Tm-Tex	$4f^{12}$	69	1.052	8.20 ± 0.01	*c*	*d*	n.m.	520	*e*	0.00126
Yb-Tex	$4f^{13}$	70	1.042	4.94 ± 0.33	827	1.498	0.126	510	22 400	0.41

[a] Ionic radii were extracted from Shannon, R. D. *Acta Crystallogr.* **1979**, *A32*, 751−767, for nine-coordinate complexes. [b] Ionic radii for eight-coordinate complexes. [c] Very weak. [d] Could not be determined. [e] No detectable absorption on the nanosecond time scale.

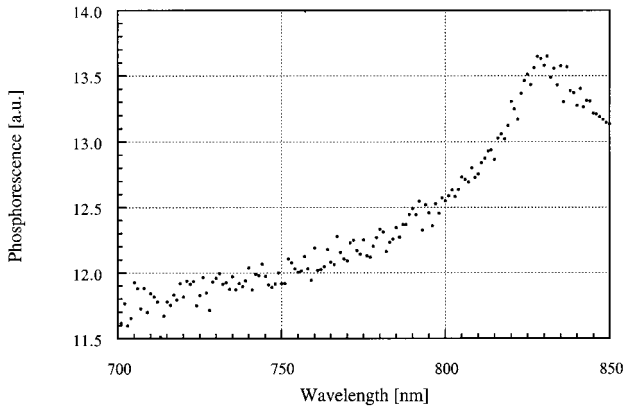

Figure 3. Phosphorescence emission of 2.0×10^{-5} M Lu-Tex in nitrogen-saturated 2-propanol solutions at 77 K; excitation wavelength 473 nm.

Phosphorescence Measurements. Metallotexaphyrins display rapid intersystem crossing from the singlet to the triplet excited state, at a rate which is competitive with that of fluorescence. For example, in an emission experiment carried out in 2-propanol at 77 K, the fluorescence of Lu-Tex was found to be quenched in the presence of iodide anion. Ablation of the fluorescence centered around 772 nm was accompanied by a new but weak band at 824 nm attributable to phosphorescence (Figure 3). Phosphorescence measurements could also be performed in aqueous solutions (5% Tween 20) by inserting a short time delay between excitation and detection. It should be noted that the latter experimental technique, which allows for a completion of the fluorescence process prior to detection, led to results completely analogous to those seen upon addition of the external heavy atom, iodide. The phosphorescence emission maxima of the other metallotexaphyrins nearly coincide with those of Lu-Tex, displaying only minor red shifts. As was the situation with the singlet excited state, coordination of different metal cations to the texaphyrin ligand appears to lead only to minor changes in triplet excited-state energies (Table 2). Unfortunately, a separate parameter of interest, the phosphorescence quantum yield, could not be compared meaningfully due to the low phosphorescence intensity ($\Phi_{PHOS} \approx 0.0001$) observed for most complexes.

Time-Resolved Measurements. Transient absorption spectra of Lu-Tex (2.0×10^{-5} M, 5% Tween 20) in oxygen-free aqueous solution, obtained 50 and 4000 ps after an 18-ps laser pulse, are shown in Figure 4. In particular, laser excitation of Lu-Tex yielded differential absorption changes in the 750−950-nm region that are dominated by strong bleaching of the ground-state absorption around 740 nm, flanked by a broad maximum at 857 nm. Thus, the immediate bleaching of the ground-state absorption, due to the conversion of the ground state to the singlet excited state, is accompanied by the generation of a new absorption attributable to singlet excited-state absorption ($^*S_1 \rightarrow {}^*S_N$).

The singlet excited-state absorption of Lu-Tex decays with clean first-order kinetics and results in the formation of a new

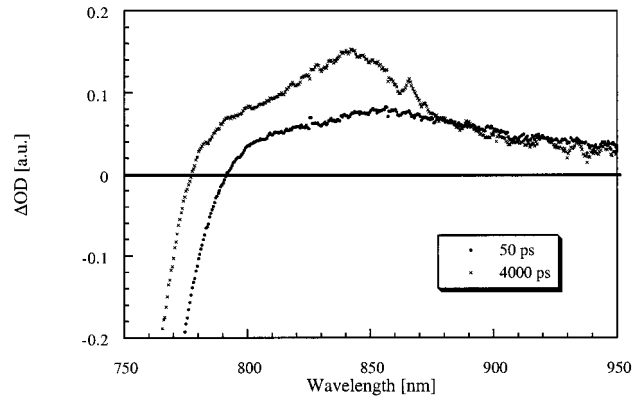

Figure 4. Transient absorption changes observed following picosecond flash photolysis (18 ps excitation pulse) at 532 nm of 2.0×10^{-5} M Lu-Tex in nitrogen-saturated aqueous solutions (5% Tween 20) at 298 K (●) 50 ps and (×) 4000 ps after the pulse.

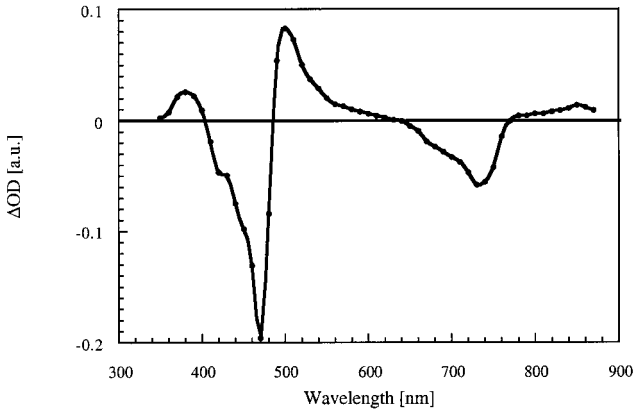

Figure 5. Transient absorption changes observed following nanosecond flash photolysis (10 ns excitation pulse) at 337 nm of 2.0×10^{-5} M Lu-Tex in nitrogen-saturated aqueous solutions (5% Tween 20) at 298 K.

absorption around 841 nm, as seen in Figure 4. This band is assigned to a triplet−triplet absorption ($T_1 \rightarrow T_N$) process. Accordingly, the grow-in of this latter absorption is indicative of intersystem crossing (ISC) between the singlet and triplet excited states. From the decay of the singlet excited-state absorption and the grow-in of the triplet−triplet absorption, an intersystem crossing rate (k_{ISC}) of 1.89×10^9 s^{-1} was calculated. The other diamagnetic texaphyrins gave rise to similar (Cd-Tex) or slower (Y-Tex, In-Tex) intersystem crossing rates, relative to those of Lu-Tex (Table 1).

Decay of the singlet excited state of the various paramagnetic metallotexaphyrin complexes also affords the corresponding T_1 triplet excited state, albeit generally at faster rates, e.g., with $k_{ISC} = 3.77 \times 10^9$ s^{-1} in the case of Gd-Tex and $k_{ISC} = 15.6 \times 10^9$ s^{-1} in the case of Dy-Tex. The rank order of ISC rates for these paramagnetic species closely resembles (but is opposite to) that found in the case of the steady-state fluorescence lifetimes, e.g., Ho(III) ≈ Dy(III) < Gd(III) < Nd(III).

Triplet Excited States. Nanosecond flash photolytic experiments were conducted using the same solute concentration as that employed in the picosecond studies (i.e., [M-Tex] = 2.0×10^{-5} M, 5% Tween 20). These measurements, designed to complement the above transient absorption studies involving the formation of the triplet excited state, were also expected to allow the decay kinetics of this state to be probed. The transient absorption spectrum of Lu-Tex, recorded 200 ns after the laser excitation at 337 nm, is shown in Figure 5. This spectrum, representative of what is seen for the other complexes studied, displays a maximum around 850 nm and strong bleaching below 770 nm. Detailed analysis of the transient absorption changes in the 750−900-nm region reveals a good spectral correlation with what is seen to develop over the course of the picosecond time regime. While it is not determined absolutely, it is therefore concluded with a high degree of certainty that no additional chemical or physical changes occur during the temporal gap between these two time regimes, i.e., between 5000 ps and 10 ns.

Analysis of the triplet−triplet spectrum ($T_1 \rightarrow T_N$) carried out over the nanosecond time domain reveals, in addition to the Q-band bleaching described above, an effective loss of absorption relative to the ground state in the region of the Soret band. Again, the coordinated metal center influences the absorbance wavelengths of the various metallotexaphyrins, but only to a very minor extent. On the other hand, as discussed immediately below, much greater effects on the rates of triplet decay were observed. The triplet absorbances generally decayed via dose-independent first-order kinetics and resulted in complete restoration of the ground state, as evidenced by full recovery of the ground-state absorption throughout the monitored wavelength region. Data concerning the triplet excited states of the investigated complexes are collected in Table 2.

As implied above, the lifetimes of the triplet excited states are strongly affected by the choice of coordinated metal center. Typically, values fall between 0.41 μs for Yb-Tex and 187 μs for Y-Tex. On the nanosecond time scale, however, laser excitation of Dy-Tex displayed no appreciable absorption changes. In particular, the characteristic triplet−triplet features, shown in Figure 5, were completely absent. Consequently, the picosecond time regime for this complex was analyzed once more in anticipation of a faster decay of the triplet excited state. From these analyses, specifically by following the decay of the transient triplet absorption after photoexcitation, a triplet lifetime of 0.94 ns was determined for Dy-Tex, a value that is markedly shorter than that of, for example, either Gd-Tex or Lu-Tex (1.11 and 35 μs, respectively; cf., Table 2).

The quantum yields of the metallotexaphyrin excited triplet states (Φ_T) were determined by the triplet−triplet energy-transfer method using a squarine dye as an energy acceptor.[32] The crown ether functionalized squarine dye was selected as the acceptor moiety, since energy transfer to this chromophore is known to be efficient.[32,33] By comparing the amount of triplet squarine dye formed in each experiment, it is possible, in principle, to determine the triplet quantum yield of a given metallotexaphyrin relative to that of a suitable standard. For the latter purpose [60]fullerene was chosen, which yields quantitative formation of the triplet excited state ($\Phi_T = 1.0$) upon photoexcitation in deoxygenated toluene solutions.[34] An additional reason for employing [60]fullerene as an internal reference is its triplet energy of 1.55 eV. As this value is comparable to those of the studied texaphyrins (1.60−1.61 eV; see Table 1), the thermodynamic driving force for the envisaged energy-transfer reactions should be similar and, in turn, ensure a meaningful comparison. Even using this approach and deoxygenated aqueous solutions, difficulties were encountered in determining the quantum yields of many of the paramagnetic systems, in part because of an inability to monitor triplet-related processes in the nanosecond regime. Of the systems that could be studied in

(32) Sauve, G.; Kamat, P. V.; Thomas, K. G.; Thomas J.; Das, S.; George, M. V. *J. Phys. Chem.* **1996**, *100*, 2117−2124.

(33) Guldi, D. M.; Liu, D.; Kamat, P. V. *J. Phys. Chem. A* **1997**, *101*, 6195−6201.

(34) Da Ros, T.; Prato, M. *Chem. Commun.* **1999**, 663−669.

Table 3. Reactivity of Triplet Excited States (^{3}*M-Tex) of Water-Soluble M-Tex Complexes with Molecular Oxygen

	electron config	atomic no.	ionic radius (Å)[a]	magnetic moment (B.M.)	lifetime (triplet, air-saturated (μs)	quenching (air-saturated) (%)	$k_{\text{singlet oxygen}}$ (M^{-1} s^{-1})	Φ_Δ
Y-Tex	$4p^6$	39	1.075	−	4.0	97.7	1.35×10^9	0.54
Cd-Tex	$4d^{10}$	48	1.10[b]	−	4.6	96.2	1.41×10^9	0.24
In-Tex	$4d^{10}$	49	0.92[b]	−	4.0	96.8	1.40×10^9	0.48
Lu-Tex	$4f^{14}$	71	1.032	−	3.5	90.1	1.30×10^9	0.31
Nd-Tex	$4f^3$	60	1.163	2.97 ± 0.02	n.m.	n.m.	n.m.	n.m.
Eu-Tex	$4f^6$	63	1.120	3.57 ± 0.11	0.51	92.7	1.38×10^9	0.09
Gd-Tex	$4f^7$	64	1.107	7.96 ± 0.15	0.83	26	1.62×10^9	0.08
Tb-Tex	$4f^8$	65	1.095	9.24 ± 0.09	*c*	*c*	*c*	*d*
Dy-Tex	$4f^9$	66	1.083	10.25 ± 0.1	*c*	*c*	*c*	*d*
Tm-Tex	$4f^{12}$	69	1.052	8.20 ± 0.01	*c*	*c*	*c*	*d*
Yb-Tex	$4f^{13}$	70	1.042	4.94 ± 0.33	0.24	58.5	1.19×10^9	0

[a] Ionic radii were extracted from Shannon, R. D. *Acta Crystallogr.* **1979**, *A32*, 751−767, for nine-coordinate complexes. [b] Ionic radii for eight-coordinate complexes. [c] No measurable effects relative to the deoxygenated solutions. [d] No detectable singlet oxygen yields.

a reliable way, rather divergent values were seen, with values ranging from $\Phi_T = 0.126$ for Yb-Tex to $\Phi_T = 0.563$ for Y-Tex (Table 2) being observed.

Singlet Oxygen Formation. Another important photophysical property of the texaphyrins involves their ability to generate singlet oxygen $^1O_2$ ($^1\Delta$) following photoexcitation under aerobic conditions.[8−15] This process, reflecting bimolecular energy transfer from the triplet excited metallotexaphyrin state to molecular oxygen, is considered to be of key importance to photodynamic therapy. Although the lifetime of triplet excited metallotexaphyrins is often shorter than those found for metalloporphyrins,[35] the strong *Q*-band absorption in the near-IR, where human tissues are most transparent,[16] makes metallotexaphyrins quite attractive as potential photosensitizers.[12−15,17,18]

The reactivity of the metallotexaphyrin triplet excited states with molecular oxygen was probed by monitoring the fate of the triplet−triplet ($T_1 \rightarrow T_N$) absorption as a function of oxygen concentration. Addition of various concentrations of oxygen in the range of $(0-1.3) \times 10^{-3}$ M to a deoxygenated solution of 2.0×10^{-5} M complex in 5% Tween 20 resulted in an accelerated decay of the triplet excited-state absorption. In all cases, the quenching of the excited states followed eq 1, where

$$k_{\text{obs}} = k_{\text{d}} + k_{\text{q}}[\text{Q}] \qquad (1)$$

k_{obs} is the observed first-order decay rate constant of the triplet excited state, k_{d} is the rate in the absence of oxygen, k_{q} is the bimolecular quenching rate constant, and [Q] is the quencher concentration (oxygen). The observed rate ($k_{\text{obs}} = \ln 2/\tau_{1/2}$) was linearly dependent on the oxygen concentration (see Figure 6), indicating that the underlying process can be attributed to a quenching of, for example,[3] (Lu-Tex) (cf., eq 2). From the slope

$$^3(\text{M-Tex}) + \text{O}_2 \xrightarrow{\text{ET}} \text{M-Tex} + {}^1\text{O}_2({}^1\Delta) \qquad (2)$$

of the plot of k_{obs} vs oxygen concentration, a value of 1.3×10^9 M^{-1} s^{-1} for k_{q} was determined for this complex. The derived rate constants for the monocationic complex Cd-Tex and dicationic complexes Y-Tex, In-Tex, Gd-Tex, and Yb-Tex appear to be very similar to that determined for Lu-Tex. Indeed, as a general rule the quenching rate constants of the water-soluble texaphyrin complexes, as summarized in Table 3, are found to be only slightly affected by the nature of the metal center. It is interesting to note that even in air-saturated solutions the diamagnetic texaphyrins display a practical triplet quenching efficiency that varies between 97.7% (Y-Tex) and 90.1% (Lu-Tex). In contrast to this, the paramagnetic Gd-Tex and Yb-Tex,

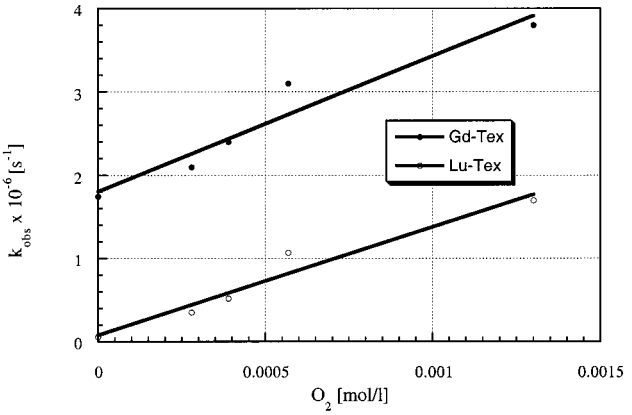

Figure 6. Plot of k_{obs} vs $[O_2]$ for the bimolecular quenching of dicationic triplet-state texaphyrin complexes ^{3}M-Tex, Gd-Tex (●) and Lu-Tex (○), by molecular oxygen, monitored at 500 nm and 510 nm, respectively.

despite yielding bimolecular quenching rate constants similar to those of the diamagnetic species (e.g., Lu-Tex, Y-Tex, In-Tex, and Cd-Tex), give rise to quenching yields of 26% and 58.5%, respectively. The rapid deactivation of the triplet excited states of the Tb-Tex, Dy-Tex, Tm-Tex, and Yb-Tex complexes prevented meaningful measurements of parameters derived from bimolecular energy-transfer studies involving molecular oxygen.

The quantum yield of singlet oxygen $^1O_2(^1\Delta)$ formation (Φ_Δ) was determined by following the emission of this latter species in the near-IR region (1270 nm). [60]Fullerene was again chosen as a model compound on the basis of the similarity between its triplet excited-state energetics and those of the water-soluble texaphyrins. In general, the quantum yield of singlet oxygen formation (Φ_Δ) closely follows the quantum yield of texaphyrin triplet excited state (Φ_T). This is consistent with the efficient bimolecular energy-transfer dynamics observed for the diamagnetic metallotexaphyrins, a process that results in a near-quantitative conversion of their triplet excited states into $^1O_2(^1\Delta)$ under conditions of appreciable oxygen tension.

Discussion

The metallotexaphyrins of this study comprise a set of analogous complexes with which to probe such fundamental questions as how the size, charge, and atomic weight of a coordinated cation influence various critical photophysical properties including fluorescent quantum yield, intersystem crossing rate, singlet- and triplet-state lifetimes, and singlet oxygen quantum yield. In the present instance, these parameters, which relate to the potential utility of a given complex in, e.g., PDT applications, could also provide an indication of the extent

(35) Kalyanasundaram, K. *Photochemistry of Polypyridine and Porphyrin Complexes*; Academic Press: London, 1992.

of covalent interaction between the texaphyrin ligand and the coordinated metal.

Given the large variety of variables which the multiplicity of photophysical parameters and range of coordinated texaphyrin cations permits one potentially to explore, we sought to find one key characteristic that could order the analysis. Here, a quick qualitative inspection of the data summarized in Tables 1−3 led to the conclusion that a clear distinction could be made, not unexpectedly, between the various diamagnetic and paramagnetic complexes. Whereas the former were characterized by relatively high fluorescent quantum yields, singlet- and triplet-state lifetimes, and singlet oxygen quantum yields, the latter were, as a rule, characterized by properties that were almost exactly converse. This broad distinction between diamagnetic and paramagnetic complexes made, it is nonetheless important to note that significant differences are seen within each of these subgroups. A discussion of these differences, their origins, and their implications, now follows.

Inspection of Table 1 reveals that among the diamagnetic complexes bearing a net +2 charge, the fluorescence quantum yield, fluorescent lifetime, and intersystem crossing rate are all correlated with atomic number. The greatest intersystem crossing rate and lowest fluorescence yield are seen for Lu-Tex, as would be expected were a heavy atom effect serving to enhance the coupling between the first excited singlet and triplet states (S_1 and T_o). In this context it is important to appreciate that X-ray structural analysis of a lutetium(III) texaphyrin analogous to that studied here revealed the metal center to be nearly within the mean texaphyrin plane with the macrocycle itself being but little distorted from planarity.[7] The observed differences are thus not ascribed to structural effects but rather to bona fide interactions between the texaphyrin ligand and metal orbitals, i.e., direct covalent effects that allow the coordinated cation to mediate the rate of $S_1 \rightarrow T_o$ spin conversion. Such considerations, however, might be less true in the case of the monocationic Cd-Tex complex. In this case, a slightly greater out-of-plane displacement is seen in the presence of a single coordinating axial ligand (0.338 Å vs 0.269 Å).[7,36]

The basic trend of the photophysical properties of diamagnetic texaphyrins being dominated by heavy atom effects holds also when the triplet-state properties of Y-Tex, In-Tex, and Lu-Tex are considered. In this instance, inspection of the available data (Table 2) reveals that both the triplet quantum yield and the triplet lifetime decrease as the atomic number increases, with, again, the monocationic Cd-Tex complex proving somewhat anomalous.

As can be seen by reference to Table 3, the relative differences in triplet quantum yield seen for the four diamagnetic complexes Y-Tex, In-Tex, Lu-Tex, and Cd-Tex correlate quite well with differences in singlet oxygen quantum yield. While slight differences in the rate of reaction with oxygen are observed for each of the relevant triplet species, as are reflected inter alia in the percentage quenching factors, the net singlet oxygen quantum yield is nevertheless highest for the lightest species, Y-Tex, and lowest for the heaviest, Lu-Tex. Interestingly, this finding is very different from what was reported by Grossweiner et al. who used an indirect approach (i.e., lysozyme inactivation) to quantum yield determination ($\Phi_\Delta = 0.29$, 0.30, 0.24, and 0.38 for Y-Tex, Cd-Tex, In-Tex, and Lu-Tex, respectively; 5% aqueous Tween 20, $\lambda_{excit} = 730$ nm).[19,37] Currently, we have no rationalization for this apparent disparity.

The photophysical behavior of the paramagnetic texaphyrin species is clearly more complex than that of their diamagnetic analogues. On the other hand, this complexity allows a number of interesting features to be noted. Most significantly, the paramagnetic complexes are seen to fluoresce weakly, with fluorescence quantum yields that are at least 1 order of magnitude smaller than those found for the corresponding diamagnetic species. A possible rationale for this difference is that the paramagnetic metal centers interact with the excited electron in the π^*-orbital and, in turn, accelerate the spin-forbidden intersystem crossing between the singlet and triplet excited states.

Looking in greater detail at the paramagnetic species, it is interesting to note that the complexes bearing the largest cations (i.e., Nd-Tex, Sm-Tex, and Eu-Tex) give rise to the lowest fluorescence quantum yields. At first glance, this appears counterintuitive, since their magnetic moments are clearly lower than that of, for example, the Ho-Tex complex. Also, the number of unpaired electrons, which might also be expected to affect the emission yields, is less than that of Gd-Tex. The Ho-Tex and Gd-Tex reveal, however, strongly enhanced emissions. This can be rationalized in terms of out-of-plane displacement particularly for the larger cations, which, in turn, should decrease the overall planarity of the complex. Since in general, decreasing the planarity of the molecule leads to poorer orbital overlap, the net result of increased out-of-plane displacement would be an overall reduction in fluorescence quantum yield, as was observed for Nd-Tex, Sm-Tex, and Eu-Tex.

Size effects in lanthanide(III) texaphyrins have been extensively studied from both structural and chemical perspectives.[7,8] One expected consequence of the variation in ionic radii for lanthanide(III) cations is that both out-of-plane displacements of the coordinated metal center and distortions of the macrocyclic framework are seen in texaphyrin complexes containing larger cations, e.g., Gd-Tex and Eu-Tex, for which an out-of-plane displacement of 0.60 Å is seen.[7,8] Thus, for these cations both the macrocyclic coordination sphere and the average metal-to-nitrogen bond length are increased. This, in turn, is expected to lower the potential overlap between the metal-based f-orbitals and the ligand-centered π-system. In previous work these structural and orbital overlap effects were shown to influence the lifetime and reactivity of the one-electron reduced metallotexaphyrin species, namely M-Tex$^{\bullet+}$ and, in the current context, are expected to play a substantial role in regulating the lifetime of the first singlet excited state, S_1.[21]

While the above effects are expected to play a substantial role in terms of modulating the various observable singlet-state properties, their influence actually pales in comparison to that associated with paramagnetism. Indeed, the shortest fluorescence lifetimes and highest intersystem crossing rates are seen for the Ho-Tex and Dy-Tex complexes, while the Nd-Tex−Tb-Tex and Er-Tex−Yb-Tex series both give rise to slower rates (Figures 7 and 8). On the other hand, a simple correlation between the observed dynamics and the number of unpaired electrons located at the metal center could not be made. For instance, while the ISC rates increase and fluorescence lifetimes decrease gradually with increasing atomic number, the Gd-Tex and Tb-Tex

(36) Sessler, J. L.; Murai, T.; Lynch, V. *Inorg. Chem.* **1989**, *28*, 1333−1341.

(37) A singlet oxygen quantum yield value for Lu-Tex of 0.73 in methanol was measured by Ehrenberg and co-workers by monitoring the rate of photosensitized diphenylisobenzofuran decomposition using tetraphenylporphyrin sulfonate as a standard: Kostenich, G.; Babushkina, T.; Lavi, A.; Langzam, Y.; Malik, Z.; Orenstein, A.; Ehrenberg, B. *J. Porphyrins Phthalocyanines* **1998**, *2*, 383−390. This value was also found to differ from that measured in methanol ($\Phi_\Delta = 0.23$) using a direct luminescence analysis.[14]

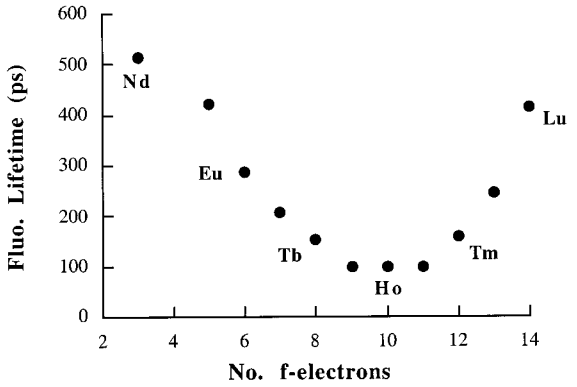

Figure 7. Plot of fluorescence lifetimes vs number of f-electrons for paramagnetic lanthanide(III) texaphyrin complexes.

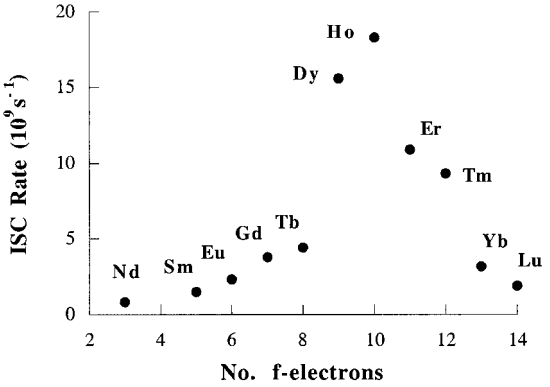

Figure 8. Plot of intersystem crossing (ISC) rate vs number of f-electrons for paramagnetic lanthanide(III) texaphyrin complexes.

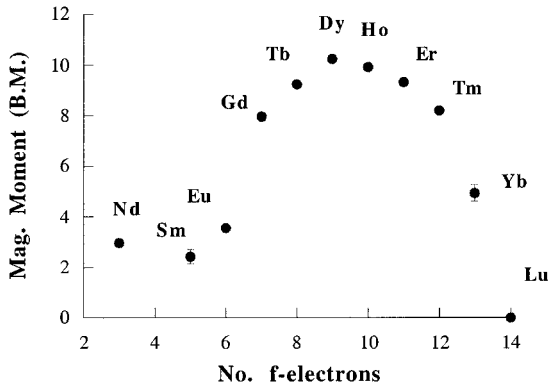

Figure 9. Plot of magnetic moments vs number of f-electrons for paramagnetic lanthanide(III) texaphyrin complexes.

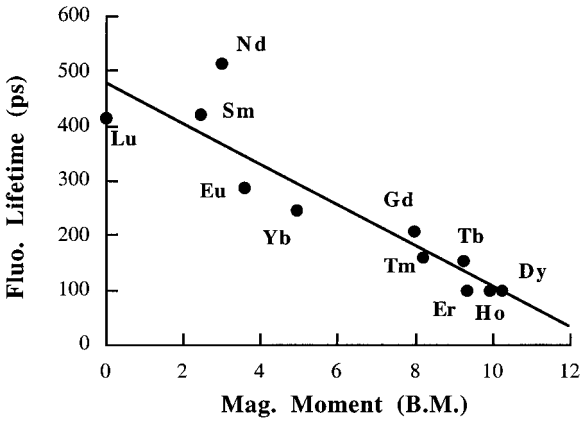

Figure 10. Plot of fluorescence lifetimes vs magnetic moments for paramagnetic lanthanide(III) texaphyrin complexes.

complexes reveal, despite having a larger number of unpaired electrons, slower ISK rates and longer lifetimes than Ho-Tex or Dy-Tex.

In contrast to what was seen with atomic number, it was found that the magnetic moments of the paramagnetic lanthnide(III) texaphyrin complexes track nicely with the fluorescence lifetimes and intersystem crossing rates (cf. Figures 9 and 10). These results are consistent with previous studies involving paramagnetic lanthanide(III) porphyrins.[1−5] These latter studies revealed, in addition to the deactivation pathways discussed herein, other effects (e.g., charge transfer and intramolecular energy transfer) arising from the presence of higher excited states (e.g., S_2). The importance of these competing pathways is lessened in the case of the texaphyrin complexes as the result of both reduced excited-state energies and a deliberate choice of lower energy excitation wavelengths.

The above experimental findings are important in that they provide additional evidence for covalent interactions between the metal f-orbitals and the p-orbitals of the texaphyrin macrocycle. This is apparent when complexes that have similar magnetic moments, but different out-of-plane displacements as the result of different cation sizes, are compared. For instance, in the Gd-Tex/Tm-Tex and Tb-Tex/Er-Tex pairs, each of the individual complexes have similar magnetic moments; however, key kinetic parameters (i.e., fluorescence lifetimes, intersystem crossing rates, and triplet lifetimes) differ dramatically. In this context, it is interesting to note that the smaller cations, which should be held more within the plane and be subject to a correspondingly greater degree of orbital overlap, show by far the fastest deactivation rates. This effect is particularly pronounced in the case of the triplet lifetimes, where a difference of nearly 3 orders of magnitude in triplet lifetimes is observed. Indeed, triplet lifetime values of 0.00126 μs and 1.11 μs are recorded for the Tm-Tex and Gd-Tex complexes, respectively. Needless to say, additional modulating factors, including those that could stem from heavy atom effects (see above discussion), cannot be ruled out at present. However, their contribution to the overall deactivation process of the excited states in the case of the paramagnetic texaphyrins is nonetheless judged to be of minor importance.

Turning to the question of singlet oxygen generation, it is found, as expected, that the short lifetimes of the triplet excited states in the paramagnetic series prevent meaningful, rate-determining reaction with molecular oxygen in most cases. Indeed, with the exception of Eu-Tex and Gd-Tex, no appreciable formation of singlet oxygen was observed within the Nd-Tex−Yb-Tex series of complexes under conditions of air saturation. While Eu-Tex and Gd-Tex do produce singlet oxygen under conditions of aerobic photoexcitation, the relevant quantum yields are, nevertheless, markedly lower than those seen in the case of the corresponding diamagnetic complexes.

Conclusion

The present study, representing one of the most comprehensive photophysical analyses hitherto carried out in the case of nonlabile lanthnide(III) complexes, has allowed a number of important trends to be highlighted. On one level, the present analyses have underscored the previous impression that the nature of the coordinated cation effects but a minimal perturbation of the relative energies of the ground, singlet, and triplet excited states.[7,21] On the other hand, the rates of excited state deactivation, as well as various quantum yields, are seen to be highly dependent on the choice of metal cation. Since these

observables reflect in part the rates of intersystem crossing and what are, in principle, spin-forbidden spin interconversion processes, it is not surprising that both heavy atom and, where relevant, paramagnetic cation effects are seen. Where applicable, the latter factor dominates, but in both cases, the fact that a dependence on metal cation is observed is consistent with there being sufficient overlap between metal-based orbitals and the ligand π-system to enhance the rate of intersystem crossing.

In general, the sum of the quantum yields, e.g., fluorescence and triplet quantum yields, is surprisingly low. This clearly points to the major role of other deactivation pathways, such as internal conversions between the respective spin states and the singlet ground state. The latter clearly compete with the emissive processes (fluorescence and phosphorescence) and intersystem crossing. In this light, Y-Tex gives rise to the most surprising observation. Although it displays the strongest S_1-derived fluorescence by far ($\Phi_F = 0.04$), it nevertheless produces its triplet excited state with the highest efficiency ($\Phi_T = 0.563$). As a consequence, ^{3}Y-Tex generates singlet oxygen ($^1O_2(^1\Delta)$) in higher quantum yield ($\Phi_\Delta = 0.54$) than any of the other species studied. From a drug development standpoint, this ability to both fluoresce in high quantum yield and produce singlet oxygen with great efficiency leads us to predict it to be a useful agent for both the photodynamic, emission-based detection of, for instance, cancerous and atheromatous disease and the subsequent light-based treatment of these same disorders. Current work is focused on exploring this promise.

Acknowledgment. This work was supported in part by the NIH (Grant No. CA 68682 to J.L.S). It was also supported in part by the Office of Basic Energy Sciences of the Department of Energy. This is document NDRL-4239 from the Notre Dame Radiation Laboratory.

JA001578B